















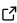
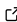
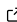
1 VOTCA: multiscale frameworks for quantum and  
2 classical simulations in soft matter

3 Björn Baumeier <sup>1,2</sup>¶, Jens Wehner <sup>1,2,3</sup>, Nicolas Renaud <sup>3</sup>, Felipe Zapata  
4 Ruiz <sup>3</sup>, Rene Halver <sup>4</sup>, Pranav Madhikar <sup>1,2</sup>, Ruben Gerritsen <sup>1,2</sup>,  
5 Gianluca Tirimbo <sup>1,2</sup>, Javier Sijen<sup>1,2</sup>, David Rosenberger <sup>5</sup>, Joshua S.  
6 Brown <sup>6</sup>, Vivek Sundaram <sup>1,2</sup>, Jakub Krajniak <sup>7</sup>, Marvin Bernhardt <sup>8</sup>,  
7 and Christoph Junghans <sup>9</sup>¶

8 1 Department of Mathematics and Computer Science, Eindhoven University of Technology, the  
9 Netherlands 2 Institute for Complex Molecular Systems, Eindhoven University of Technology, the  
10 Netherlands 3 Netherlands eScience Center, the Netherlands 4 Forschungszentrum Jülich, Jülich,  
11 Germany 5 Freie Universität Berlin, Berlin, Germany 6 Oak Ridge National Laboratory, Oak Ridge, TN,  
12 USA 7 Katholieke Universiteit Leuven, Leuven, Belgium 8 Technische Universität Darmstadt, Darmstadt,  
13 Germany 9 Los Alamos National Laboratory, Los Alamos, New Mexico, USA ¶ Corresponding author

DOI: [10.xxxxxx/draft](https://doi.org/10.xxxxxx/draft)

Software

- [Review](#) 
- [Repository](#) 
- [Archive](#) 

Editor: 

Submitted: 27 May 2024

Published: unpublished

License

Authors of papers retain copyright  
and release the work under a  
Creative Commons Attribution 4.0  
International License ([CC BY 4.0](https://creativecommons.org/licenses/by/4.0/)).

14 **Summary**

15 Many physical phenomena in liquids and soft matter are multiscale by nature and can involve  
16 processes with quantum and classical degrees of freedom occurring over a vast range of length-  
17 and timescales. Examples range from structure formation processes of complex polymers  
18 or even polymer blends on the classical side to charge and energy transport and conversion  
19 processes involving explicit electronic and therefore quantum information.

20 The Versatile Object-Oriented Toolkit for Coarse-graining Applications (VOTCA) provides  
21 multiscale frameworks built on a comprehensive set of methods for the development of  
22 classical coarse-grained potentials (VOTCA-CSG) as well as state-of-the art excited state  
23 electronic structure methods based on density-functional and many-body Green's function  
24 theories, coupled in mixed quantum-classical models and used in kinetic network models  
25 (VOTCA-XTP).

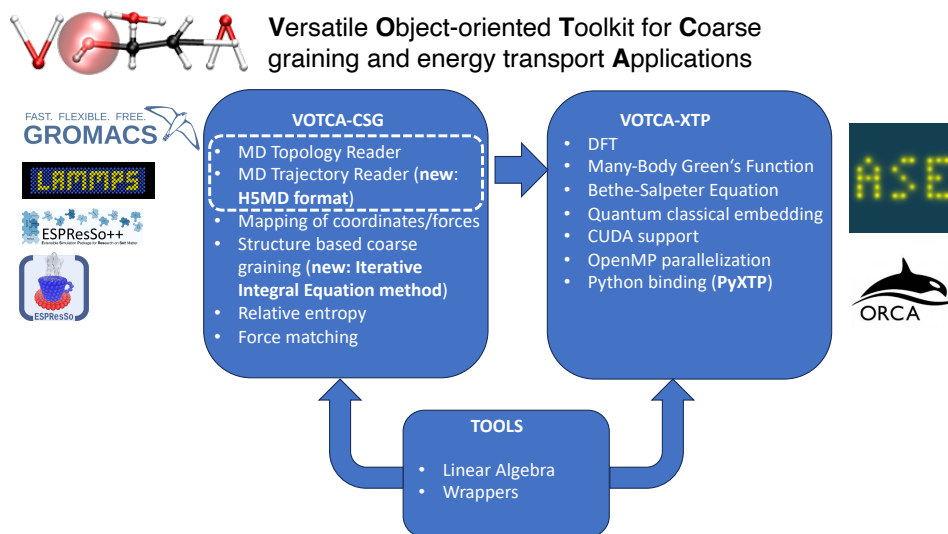


**Figure 1:** Overview of the different VOTCA modules and external interfaces. The trajectory reader of VOTCA-CSG in the dashed line box are reused by VOTCA-XTP.

## 26 Statement of need

27 VOTCA was originally developed as a platform for development and comparison of coarse-  
 28 graining (CSG) methods. Since the last software publication in 2015 VOTCA-CSG was  
 29 strengthened by adding more methods, more examples and involving more developers. Many  
 30 users have used VOTCA to compare different coarse-graining strategies on a neutral ground  
 31 and, if needed, proceeded with a more specialized package based on the gained insight. Such  
 32 other coarse-graining packages include, among others, BOCS (Dunn et al., 2018), DeePCG  
 33 (Zhang et al., 2018), IBIsCO (Karimi-Varzaneh et al., 2011), MagiC (Mirzoev & Lyubartsev,  
 34 2013) and OpenMSCG (Peng et al., 2023), some of which are not open-source or specialized  
 35 in one method. Others have stopped being developed or lack contributions from the greater  
 36 community. It is difficult to build all-inclusive community package for coarse-graining as it is  
 37 sometimes hard to consolidate different development styles and constantly changing priorities  
 38 from sponsors that leave little time for good software engineering practices. In this context  
 39 we would like to point out that there is a fork of the VOTCA package ([mpip-votca?](#)) that  
 40 contains some feature e.g. Kernel-based machine learning methods (Scherer et al., 2020), that  
 41 has not been merged.

42 Next to strengthening the coarse-graining functionality of VOTCA, another major development  
 43 direction taken since 2015 is the addition of explicit quantum-mechanical modules aiming at the  
 44 simulation of static and dynamic properties of electronically excited states in complex molecular  
 45 environments using multiscale frameworks. Specifically, the VOTCA-XTP part provides an  
 46 open-source implementation of many-body Green's functions methods (known as *GW*-BSE)  
 47 with the capability of linking this quantum-mechanical description of a molecular system  
 48 to a classical (microelectrostatic) environment model and to perform rate-based dynamic  
 49 simulations with kinetic Monte-Carlo. Basic *GW*-BSE functionality in molecular settings has  
 50 also more recently been supported in other packages, such as Turbomole (Balasubramani et  
 51 al., 2020), ADF (Velde et al., 2001), PySCF (Sun et al., 2020), or MOLGW (Bruneval et al.,  
 52 2016), but these are either commercial or do not provide links to a multiscale framework for  
 53 complex environments and dynamics.

54 **Coarse-Graining**

55 In the coarse-graining part of VOTCA, VOTCA-CSG, we made a lot of improvements to the  
56 inverse Monte Carlo (IMC) method and have added a new iterative approach the so-called  
57 iterative integral equation (IIE) method, which are both described in detail below and in  
58 reference therein.

59 **Inverse Monte Carlo updates**

60 The inverse Monte-Carlo Method introduced by Lyubartsev and Laaksonen in 1995 (A. P.  
61 Lyubartsev & Laaksonen, 1995) is a structure-based coarse graining method, whose goal it is  
62 to find an effective pair potential between particles, which reproduces the radial distribution  
63 function (RDF) of a reference system (ref) at the coarse grained (CG) resolution. IMC has  
64 been part of VOTCA since its first release. In the original implementation the pair potential  
65 was determined by iteratively solving a set of linear equations:

$$(A^T A) \Delta U_{ij} = A^T (g_{ij}^{n-1} - g_{ij}^{ref}), \quad (1)$$

66 where  $g_{ij}$  is the RDF between particles  $i$  and  $j$ ,  $n$  indicates the iteration counter,  $\Delta U_{ij}$  is the  
67 potential update term, and  $A$  and  $A^T$  are the Jacobian and its corresponding transpose. The  
68 Jacobian  $A$  is defined as:

$$A = \frac{\partial g_{ij}}{\partial U_{ij}}, \quad (2)$$

69 where  $U_{ij}$  is the pair potential between particles  $i$  and  $j$ .

70 Rosenberger *et al.* (Rosenberger *et al.*, 2016), among others (A. Lyubartsev *et al.*, 2010;  
71 Murtola *et al.*, 2007; Tóth, 2003), demonstrated that the standard IMC method can suffer  
72 from numerical instabilities and/or slow convergence. Therefore, a Tikhonov regularization  
73 for IMC has been implemented in VOTCA. This regularization changes the linear equations  
74 according to (Rosenberger *et al.*, 2016):

$$(A^T A + \lambda I) \Delta U_{ij} = A^T (g_{ij}^{n-1} - g_{ij}^{ref}), \quad (3)$$

75 where  $\lambda$  determines the strength of the regularization and  $I$  is the identity matrix. One can  
76 perform a singular value decomposition of the Jacobian  $A$  to determine an initial value for  
77  $\lambda$  (Rosenberger *et al.*, 2016). As a rule of thumb  $\lambda$  should at least be at the order of the  
78 smallest singular values squared.

79 **Iterative Integral Equation method**

80 The iterative integral equation methods are similar to IMC in that they also aim at reconstructing  
81 the RDF of a fine-grained reference system with an effective pair potential. The main difference  
82 is in the construction of the Jacobian, which is approximated in IIE methods from integral  
83 equation theory. (Delbary *et al.*, 2020) For a molecular fluid, where each molecule is mapped to  
84 a single bead, using the Ornstein-Zernicke equation and the hypernetted-chain closure, one  
85 arrives at the Jacobian inverse with the form of

$$A^{-1} = \frac{dU}{dg} = \frac{1}{\beta} \left( 1 - \frac{1}{g} - \mathcal{F}^{-1} \left( \frac{1}{(1 + \rho \hat{h})^2} \right) \mathcal{F} \right). \quad (4)$$

86 Here,  $\hat{h}$  is the Fourier transform of  $h = g - 1$  and  $\mathcal{F}$  is the Fourier operator. This approximate  
87 Jacobian works well for systems with single-bead molecule representations with convergence as  
88 fast as IMC, whereas in the general case, convergence is half as fast as IMC. (Bernhardt *et al.*,  
89 2023) The costly sampling of the IMC Matrix is not needed, only an RDF which is calculated  
90 on twice the range as the potential. (Bernhardt *et al.*, 2021)

91 **Constraints**

92 When using the IMC or IIE methods described above to find pair potentials, that best reproduce  
 93 a reference RDF, one can use the Gauss-Newton algorithm and formulate the problem of  
 94 finding a potential update  $\Delta U$  as a minimization

$$\arg \min_{\Delta U} \|\Delta g + A\Delta U\|_2 \quad (5)$$

95 where  $\Delta g = g - g_{\text{target}}$ . In that case, additional constraints can be introduced. For example,  
 96 it is possible to describe the pressure of a system in terms of the RDF  $g$  and the pair potential  
 97  $U$ . From a target pressure and the current pressure at each iteration, a constraint of the form  
 98  $B\Delta U = d$  can be described and the constraint is enforced by elimination. (Bernhardt et al.,  
 99 2021)

100 **Electronic Excitations**

101 The most substantial new feature in the VOTCA package is the addition of explicit quantum-  
 102 mechanical functionalities in the VOTCA-XTP part. The added methods aim at a first-  
 103 principles-based multiscale modeling of electronically excited states and their dynamics in  
 104 complex molecular systems. We very briefly describe the three main modules of XTP in the  
 105 following.

106 **Density-Functional Theory**

107 Excited state calculations require a reference ground state calculation within density-functional  
 108 theory. VOTCA-XTP provides both an automated interface to the ORCA package (Neese,  
 109 2012) and a lightweight internal DFT engine based on atom-centered Gaussian-type orbitals  
 110 for method developing and testing. It solves the Kohn-Sham Equations for the molecular orbitals  
 111  $\phi_n^{\text{KS}}(\mathbf{r})$  with orbital energies  $\varepsilon_n^{\text{KS}}$

$$\left\{ -\frac{\hbar^2}{2m} \nabla^2 + V_{\text{ext}}(\mathbf{r}) + V_{\text{H}}(\mathbf{r}) + V_{\text{xc}}(\mathbf{r}) \right\} \phi_n^{\text{KS}}(\mathbf{r}) = \varepsilon_n^{\text{KS}} \phi_n^{\text{KS}}(\mathbf{r}), \quad (6)$$

112 where  $V_{\text{ext}}$  is the external potential,  $V_{\text{H}}$  the Hartree potential, and  $V_{\text{xc}}$  the exchange-correlation  
 113 potential. VOTCA-XTP also contains functionality for projector-based-embedding DFT-in-  
 114 DFT ground state calculations (Manby et al., 2012), in which a chosen *active* subregion of a  
 115 molecular system is embedded into an inactive one, reproducing the total energy of the full  
 116 system ground state exactly.

117 **Many-Body Green's Functions and the Bethe-Salpeter Equation**

118 Using the ground-state reference, many-body Green's functions theory with the *GW* approxi-  
 119 mation first calculates *single-particle excitations* (electron addition or removal) as solutions to  
 120 the *quasiparticle equations*

$$\left\{ -\frac{\hbar^2}{2m} \nabla^2 + V_{\text{ext}}(\mathbf{r}) + V_{\text{H}}(\mathbf{r}) \right\} \phi_n^{\text{QP}}(\mathbf{r}) + \int \Sigma(\mathbf{r}, \mathbf{r}', \varepsilon_n^{\text{QP}}) \phi_n^{\text{QP}}(\mathbf{r}') d\mathbf{r}' = \varepsilon_n^{\text{QP}} \phi_n^{\text{QP}}(\mathbf{r}). \quad (7)$$

121 In place of the exchange-correlation potential in Eq.6, the energy-dependent self-energy operator  
 122  $\Sigma(\mathbf{r}, \mathbf{r}', E)$  occurs in the QP equations. This operator is evaluated using the one-body Green's  
 123 function in quasi-particle approximation

$$G(\mathbf{r}, \mathbf{r}', \omega) = \sum_n \frac{\phi_n(\mathbf{r}) \phi_n^*(\mathbf{r}')}{\omega - \varepsilon_n + i0^+ \text{sgn}(\varepsilon_n - \mu)} \quad (8)$$

124 as

$$\Sigma(\mathbf{r}, \mathbf{r}', E) = \frac{i}{2\pi} \int e^{-i\omega 0^+} G(\mathbf{r}, \mathbf{r}', E - \omega) W(\mathbf{r}, \mathbf{r}', \omega) d\omega, \quad (9)$$

125 where  $W$  denotes the dynamically screened Coulomb interaction. Assuming that  $\phi_n^{\text{QP}} \approx \phi_n^{\text{KS}}$ ,  
 126 the quasiparticle energies can be evaluated perturbatively according to

$$\varepsilon_n^{\text{QP}} = \varepsilon_n^{\text{KS}} + \Delta\varepsilon_n^{\text{GW}} = \varepsilon_n^{\text{KS}} + \langle \phi_n^{\text{KS}} | \Sigma(\varepsilon_n^{\text{QP}}) - V_{\text{xc}} | \phi_n^{\text{KS}} \rangle. \quad (10)$$

127 As the correction  $\Delta\varepsilon_n^{\text{GW}}$  itself depends on  $\varepsilon_n^{\text{QP}}$ , Eq.10 needs to be solved self-consistently.

128 Neutral excitations with a conserved number of electrons can be obtained from the Bethe-  
 129 Salpeter Equation (BSE) by expressing coupled electron-hole amplitudes of excitation  $S$  in a  
 130 product basis of single-particle orbitals, i.e.,

$$\chi_S(\mathbf{r}_e, \mathbf{r}_h) = \sum_v^{\text{occ}} \sum_c^{\text{unocc}} A_{vc}^S \phi_c(\mathbf{r}_e) \phi_v^*(\mathbf{r}_h) + B_{vc}^S \phi_v(\mathbf{r}_e) \phi_c^*(\mathbf{r}_h), \quad (11)$$

131 where  $\mathbf{r}_e$  ( $\mathbf{r}_h$ ) is for the electron (hole) coordinate and  $A_{vc}$  ( $B_{vc}$ ) are the expansion coefficients  
 132 of the excited state wave function in terms of resonant (anti-resonant) transitions between  
 133 occupied  $v$  and unoccupied  $c$  states, respectively. In this basis, the BSE turns into an effective  
 134 two-particle Hamiltonian problem of the form

$$\begin{pmatrix} \underline{\mathbf{H}}^{\text{res}} & \underline{\mathbf{K}} \\ -\underline{\mathbf{K}} & -\underline{\mathbf{H}}^{\text{res}} \end{pmatrix} \begin{pmatrix} \mathbf{A}^S \\ \mathbf{B}^S \end{pmatrix} = \Omega_S \begin{pmatrix} \mathbf{A}^S \\ \mathbf{B}^S \end{pmatrix}. \quad (12)$$

135 Specifically, the matrix elements of the blocks  $\underline{\mathbf{H}}^{\text{res}}$  and  $\underline{\mathbf{K}}$  are calculated as

$$H_{vc,v'c'}^{\text{res}} = D_{vc,v'c'} + \eta K_{vc,v'c'}^{\text{x}} + K_{vc,v'c'}^{\text{d}} \quad (13)$$

$$K_{cv,v'c'} = \eta K_{cv,v'c'}^{\text{x}} + K_{cv,v'c'}^{\text{d}}, \quad (14)$$

136 with

$$D_{vc,v'c'} = (\varepsilon_c - \varepsilon_v) \delta_{vv'} \delta_{cc'}, \quad (15)$$

$$K_{vc,v'c'}^{\text{x}} = \iint \phi_c^*(\mathbf{r}_e) \phi_v(\mathbf{r}_e) v_C(\mathbf{r}_e, \mathbf{r}_h) \phi_{c'}(\mathbf{r}_h) \phi_{v'}^*(\mathbf{r}_h) d^3\mathbf{r}_e d^3\mathbf{r}_h \quad (16)$$

$$K_{vc,v'c'}^{\text{d}} = - \iint \phi_c^*(\mathbf{r}_e) \phi_{c'}(\mathbf{r}_e) W(\mathbf{r}_e, \mathbf{r}_h, \omega = 0) \phi_v(\mathbf{r}_h) \phi_{v'}^*(\mathbf{r}_h) d^3\mathbf{r}_e d^3\mathbf{r}_h. \quad (17)$$

137 and  $\eta = 2$  ( $\eta = 0$ ) for singlet (triplet) excitations. Here,  $K^{\text{x}}$  is the repulsive exchange  
 138 interaction originating from the bare Coulomb term  $v_C$ , while the direct interaction  $K^{\text{d}}$   
 139 contains the attractive, but screened, interaction  $W$  between electron and hole, causing the  
 140 binding of the electron-hole pair. In Eq.17 it is assumed that the dynamic properties of  $W(\omega)$   
 141 are negligible, and the computationally less demanding static approximation  $\omega = 0$  is employed.

## 142 Quantum-Classical Embedding

143 Polarization effects of an environment can have significant impact on electronic excitations.  
 144 As polarization effects are long-ranged accounting for them requires the treatment of large  
 145 systems which is infeasible with explicit quantum methods such as DFT-GW-BSE. Instead,  
 146 the system is split into a small part with to electronically active subsystem to be treated at  
 147 quantum (QM) level and a large environment part in which electrostatic and polarization  
 148 effects are accounted for in classical models (MM). In VOTCA-XTP the QM/MM scheme  
 149 employs distributed atomic multipole representations for molecules in the MM region, which  
 150 allows treatment of both the effects of static electric fields and the polarization response as a  
 151 self-consistent reaction field. Specifically, this classical MM energy for the system is evaluated  
 152 as

$$E_{\text{MM}} = \frac{1}{2} \sum_{\substack{A,B \\ A \neq B}} \sum_{a \in A} \sum_{b \in B} \sum_{tu} (Q_t^a + \Delta Q_t^a) T_{tu}^{ab} Q_u^b, \quad (18)$$

153 where  $A$  and  $B$  indicate individual molecules in the system,  $a$  and  $b$  atoms in the respective  
154 molecules,  $Q_t^a$  are the static atomic multipole moments of rank  $t$  associated to atom  $a$ , and  
155  $T_{tu}^{ab}$  is the tensor describing the interactions between the multipoles moments  $Q_t^a$  and  $Q_u^b$   
156 (Stone, 2005). The induced moments  $\Delta Q_t^a$  are generated by the electric field created by  
157 moments  $t'$  of atom  $a' \neq a$  in molecule  $A$  and the one generated by the moment  $u$  of atom  $b$   
158 in molecule  $B$ :

$$\Delta Q_t^a = - \sum_{\substack{A, B \in \mathcal{S} \\ A \neq B}} \sum_{b \in B} \sum_{\substack{a' \in A \\ a' \neq a}} \sum_{tt'u} \alpha_{tt'}^{aa'} T_{t'u}^{a'b} (Q_u^b + \Delta Q_u^b), \quad (19)$$

159 with  $\alpha_{tt'}^{aa'}$  the isotropic atomic polarizability on each site. To avoid effects of spurious  
160 overpolarization, a damped version of the interaction tensor (Thole damping (Stone, 2005))  
161 is used. Then, the static and induced multipoles in the MM region also interact with the  
162 electron density in QM region via an additional external potential to Eq.6. At the same time,  
163 the explicit electrostatic field from the QM density is included in polarizing the MM region.

## 164 Code Structure

165 For the last couple of years, we have also focused on code hardening and the introduction of  
166 better software engineering practices. Original VOTCA was designed as modules in separate  
167 repositories, but as many other projects, this turned out to be quite cumbersome hence we  
168 switched to a mono-repo. With recent performance improvements in the git tools, the benefits  
169 of a single repository by far out-weigh the downside of the very complex workflow of multiple  
170 repositories. The module structure still exists in the source code.

171 Additionally, we have added continuous integration testing through GitHub action for 50+  
172 different compiler and operating system combinations. We also perform continuous deployment  
173 to the GitHub Docker registry. And releases get rolled into all major linux distributions,  
174 HomeBrew, Spack and FreeBSD.

## 175 Code Modernization

176 We did a lot of code refactoring and bumped the C++ standard to 17. We also modernized  
177 our usage of CMake and switched to a mostly target-base scheme. An attempt to port our  
178 particle structure on top of Cabana (Slattery et al., 2022) was made, due to incompatibilities  
179 between Kokkos (Trott et al., 2022) and Eigen, we will delay this effort.

## 180 Updates in VOTCA-CSG

181 The particle and molecule data structure were refactored, and we add support of the H5MD  
182 format, which is described below in details.

### 183 H5MD support

184 The recent version of VOTCA supports the H5MD (de Buyl et al., 2014) file format, which  
185 internally uses HDF5 (The HDF Group, n.d.) storage. This is a very fast and scalable method  
186 for storing molecular trajectories, already implemented in simulation packages such as LAMMPS,  
187 ESPResSo++, and ESPResSo. VOTCA recognizes the trajectory file format by the extension. In  
188 the case of H5MD, it expects a .h5 extension. Following the H5MD concepts, the particle  
189 trajectories are organized in the particles container. This container can handle multiple  
190 subsets of the studied system. Therefore, we must define h5md\_particle\_group in the XML  
191 topology file to declare which subset of particles to use. The reader handles both coordinates  
192 (if present), forces, and velocities.

## 193 Design of VOTCA-XTP

194 Data structures related to atomistic properties (topology, molecules, segments, fragments,  
195 atoms) in XTP are reused or build upon those of CSG. Linear algebra related structures and  
196 functionalities are handled by Eigen (Guennebaud et al., 2010) which can be accelerated by  
197 internally calling the Intel Math Kernel Library (*Intel Math Kernel Library. Reference Manual,*  
198 2009). Exchange-correlation functionals are provided by the Library of eXchange-Correlation  
199 (LIBXC) functionals (Lehtola et al., 2018), while libint (Valeev, 2024) and libecpint (Shaw  
200 & Hill, 2017) are used for the evaluation of molecular integrals of many-body operators over  
201 Gaussian functions.

202 VOTCA-XTP is designed as a library, which is linked to very thin executables. These executables  
203 provide a variety of calculators by adding keywords on the command line. Virtual interfaces  
204 and factory patterns make the addition of new calculators simple. The same architecture is  
205 used for external DFT and MD codes, making VOTCA-XTP easily extensible. Lower-level  
206 data structures make use of template metaprogramming to support a variety of data types.  
207 VOTCA-XTP provides different functionalities in three types of *calculator* classes:

- 208 ■ a collection of tools that do not require information of a mapped MD trajectory, including  
209 a specific DFT-*GW*-BSE calculator in `tools` callable by `xtp_tools`
- 210 ■ analysis and not-high-throughput applications that require a mapped MD trajectory in  
211 `calculators` callable by `xtp_run`
- 212 ■ high-throughput, high-performance applications that require a mapped MD trajectory in  
213 `jobcalculators` callable by `xtp_parallel`

214 In general, VOTCA-XTP uses shared-memory parallelization in the heavy calculations involving  
215 the quantum methods, with the possibility to seamlessly offload matrix-matrix and matrix-vector  
216 operations to GPU via CUDA.

## 217 PyXTP

218 The PyXTP python package distributed with VOTCA, contains python bindings to the main  
219 functionalities of VOTCA-XTP. These python bindings were created using pybind11 (Jakob  
220 et al., 2017) and provide users with a dedicated Atomistic Simulation Environment (ASE)  
221 (Larsen et al., 2017) calculator. The use of this calculator not only facilitates the adoption  
222 of VOTCA-XTP by non-experts users, but they also allow integrating VOTCA-XTP in the  
223 broader ASE ecosystem.

224 The following snippet of code illustrate the use of PyXTP. This small code optimize the  
225 geometry of a CO molecule in the first excited singlet states. As seen in the code, the XTP  
226 calculator is used to compute the forces on the nuclei while the geometry optimization itself is  
227 driven by ASE functionalities.

```
from pyxtp import xtp
from ase.io import write
from ase.build import molecule
from ase.optimize import QuasiNewton

# create a distorted CO molecule
atoms = molecule('CO')
atoms.rattle()

# instantiate the calculator
calc = xtp(nthreads=2)

# select the state for which to compute the forces
calc.select_force(energy='singlets', level=0, dynamic=False)
```

```
# this allows to change all options
calc.options.dftpackage.functional = 'PBE'
calc.options.dftpackage.basisset = 'def2-svp'
calc.options.dftpackage.auxbasisset = 'aux-def2-svp'

# set up the logger
calc.options.logging_file = 'CO_forces.log'

# set the calculator
atoms.calc = calc

# optimize the geometry
dyn = QuasiNewton(atoms, trajectory='test.traj')
dyn.run(fmax=0.01)
write('final.xyz', atoms)
```

## 228 Acknowledgements

229 We acknowledge contributions from Brigitta Sipocz, Syrtis Major, and Semyeong Oh, and  
230 support from Kathryn Johnston during the genesis of this project. We acknowledge support by  
231 the Innovational Research Incentives Scheme Vidi of the Netherlands Organisation for Scientific  
232 Research (NWO) with project number 723.016.002. Funding is also provided by NWO and  
233 the Netherlands eScience Center for funding through project number 027.017.G15, within the  
234 Joint CSER and eScience program for Energy Research (JCER 2017).

## 235 References

- 236 Balasubramani, S. G., Chen, G. P., Coriani, S., Diedenhofen, M., Frank, M. S., Franzke, Y. J.,  
237 Furche, F., Grotjahn, R., Harding, M. E., Hättig, C., Hellweg, A., Helmich-Paris, B., Holzer,  
238 C., Huniar, U., Kaupp, M., Marefat Khah, A., Karbalaei Khani, S., Müller, T., Mack, F., ...  
239 Yu, J. M. (2020). TURBOMOLE: Modular program suite for ab initio quantum-chemical  
240 and condensed-matter simulations. *The Journal of Chemical Physics*, 152(18), 184107.  
241 <https://doi.org/10.1063/5.0004635>
- 242 Bernhardt, M. P., Hanke, M., & Van Der Vegt, N. F. A. (2023). Stability, speed, and  
243 constraints for structural coarse-graining in VOTCA. *Journal of Chemical Theory and  
244 Computation*, 19(2), 580–595. <https://doi.org/10.1021/acs.jctc.2c00665>
- 245 Bernhardt, M. P., Hanke, M., & Vegt, N. F. A. van der. (2021). Iterative integral equation  
246 methods for structural coarse-graining. *The Journal of Chemical Physics*, 154(8), 084118.  
247 <https://doi.org/10.1063/5.0038633>
- 248 Bruneval, F., Rangel, T., Hamed, S. M., Shao, M., Yang, C., & Neaton, J. B. (2016). Molgw  
249 1: Many-body perturbation theory software for atoms, molecules, and clusters. *Computer  
250 Physics Communications*, 208, 149–161. <https://doi.org/https://doi.org/10.1016/j.cpc.2016.06.019>
- 251
- 252 de Buyl, P., Colberg, P. H., & Höfling, F. (2014). H5MD: A structured, efficient, and portable  
253 file format for molecular data. *Computer Physics Communications*, 185(6), 1546–1553.  
254 <https://doi.org/https://doi.org/10.1016/j.cpc.2014.01.018>
- 255 Delbary, F., Hanke, M., & Ivanizki, D. (2020). A generalized newton iteration for computing  
256 the solution of the inverse henderson problem. *Inverse Problems in Science and Engineering*,  
257 28(8), 1166–1190. <https://doi.org/10.1080/17415977.2019.1710504>



- 258 Dunn, N. J. H., Lebold, K. M., DeLyser, M. R., Rudzinski, J. F., & Noid, W. G. (2018). BOCS:  
259 Bottom-up open-source coarse-graining software. *The Journal of Physical Chemistry B*,  
260 122(13), 3363–3377. <https://doi.org/10.1021/acs.jpcc.7b09993>
- 261 Guennebaud, G., Jacob, B., & others. (2010). *Eigen v3*. <http://eigen.tuxfamily.org>.
- 262 *Intel Math Kernel Library. Reference Manual*. (2009). [Computer software]. Intel Corporation.
- 263 Jakob, W., Rhineland, J., & Moldovan, D. (2017). *pybind11 – seamless operability between*  
264 *c++11 and python*.
- 265 Karimi-Varzaneh, H. A., Qian, H.-J., Chen, X., Carbone, P., & Müller-Plathe, F. (2011).  
266 IBIsCO: A molecular dynamics simulation package for coarse-grained simulation. *Journal*  
267 *of Computational Chemistry*, 32(7), 1475–1487. [https://doi.org/10.1002/](https://doi.org/10.1002/jcc.21717)  
268 [jcc.21717](https://doi.org/10.1002/jcc.21717)
- 269 Larsen, A. H., Mortensen, J. J., Blomqvist, J., Castelli, I. E., Christensen, R., Duřak, M.,  
270 Friis, J., Groves, M. N., Hammer, B., Hargus, C., Hermes, E. D., Jennings, P. C.,  
271 Jensen, P. B., Kermode, J., Kitchin, J. R., Kolsbjerg, E. L., Kubal, J., Kaasbjerg, K.,  
272 Lysgaard, S., ... Jacobsen, K. W. (2017). The atomic simulation environment—a python  
273 library for working with atoms. *Journal of Physics: Condensed Matter*, 29(27), 273002.  
274 <http://stacks.iop.org/0953-8984/29/i=27/a=273002>
- 275 Lehtola, S., Steigemann, C., Oliveira, M. J. T., & Marques, M. A. L. (2018). Recent  
276 developments in LIBXC — A comprehensive library of functionals for density functional  
277 theory. *SoftwareX*, 7, 1–5. <https://doi.org/10.1016/j.softx.2017.11.002>
- 278 Lyubartsev, A. P., & Laaksonen, A. (1995). Calculation of effective interaction potentials from  
279 radial distribution functions: A reverse Monte Carlo approach. *Physical Review E*, 52(4),  
280 3730–3737. <https://doi.org/10.1103/PhysRevE.52.3730>
- 281 Lyubartsev, A., Mirzoev, A., Chen, L., & Laaksonen, A. (2010). Systematic coarse-graining  
282 of molecular models by the Newton inversion method. *Faraday Discuss.*, 144, 43–56.  
283 <https://doi.org/10.1039/B901511F>
- 284 Manby, F. R., Stella, M., Goodpaster, J. D., & Miller, T. F. (2012). A simple, exact  
285 density-functional-theory embedding scheme. *J. Chem. Theory Comput.*, 8, 2564–2568.
- 286 Mirzoev, A., & Lyubartsev, A. P. (2013). MagiC: Software package for multiscale modeling.  
287 *Journal of Chemical Theory and Computation*, 9(3), 1512–1520. [https://doi.org/10.1021/](https://doi.org/10.1021/ct301019v)  
288 [ct301019v](https://doi.org/10.1021/ct301019v)
- 289 Murtola, T., Falck, E., Karttunen, M., & Vattulainen, I. (2007). Coarse-grained model  
290 for phospholipid/cholesterol bilayer employing inverse Monte Carlo with thermodynamic  
291 constraints. *The Journal of Chemical Physics*, 126(7), 075101. [https://doi.org/10.1063/1.](https://doi.org/10.1063/1.2646614)  
292 [2646614](https://doi.org/10.1063/1.2646614)
- 293 Neese, F. (2012). The ORCA program system. *WIREs Computational Molecular Science*, 2(1),  
294 73–78. <https://doi.org/10.1002/wcms.81>
- 295 Peng, Y., Pak, A. J., Durumeric, A. E. P., Sahrman, P. G., Mani, S., Jin, J., Loose,  
296 T. D., Beiter, J., & Voth, G. A. (2023). OpenMSCG: A software tool for bottom-  
297 up coarse-graining. *The Journal of Physical Chemistry B*, 127(40), 8537–8550. <https://doi.org/10.1021/acs.jpcc.3c04473>  
298 [/doi.org/10.1021/acs.jpcc.3c04473](https://doi.org/10.1021/acs.jpcc.3c04473)
- 299 Rosenberger, D., Hanke, M., & Vegt, N. F. A. van der. (2016). Comparison of iterative  
300 inverse coarse-graining methods. *The European Physical Journal Special Topics*, 225(8-9),  
301 1323–1345. <https://doi.org/10.1140/epjst/e2016-60120-1>
- 302 Scherer, C., Scheid, R., Andrienko, D., & Bereau, T. (2020). Kernel-based machine learning  
303 for efficient simulations of molecular liquids. *Journal of Chemical Theory and Computation*,  
304 16(5), 3194–3204. <https://doi.org/10.1021/acs.jctc.9b01256>

- 305 Shaw, R. A., & Hill, J. G. (2017). Prescreening and efficiency in the evaluation of integrals  
306 over ab initio effective core potentials. *The Journal of Chemical Physics*, 147(7), 074108.  
307 <https://doi.org/10.1063/1.4986887>
- 308 Slattery, S., Reeve, S. T., Junghans, C., Lebrun-Grandié, D., Bird, R., Chen, G., Fogerty, S.,  
309 Qiu, Y., Schulz, S., Scheinberg, A., Isner, A., Chong, K., Moore, S., Germann, T., Belak,  
310 J., & Mniszewski, S. (2022). Cabana: A performance portable library for particle-based  
311 simulations. *Journal of Open Source Software*, 7(72), 4115. [https://doi.org/10.21105/  
312 joss.04115](https://doi.org/10.21105/joss.04115)
- 313 Stone, A. J. (2005). Distributed Multipole Analysis: Stability for Large Basis Sets. *Journal of*  
314 *Chemical Theory and Computation*, 1(6), 1128–1132. <https://doi.org/10.1021/ct050190+>
- 315 Sun, Q., Zhang, X., Banerjee, S., Bao, P., Barbry, M., Blunt, N. S., Bogdanov, N. A., Booth,  
316 G. H., Chen, J., Cui, Z.-H., Eriksen, J. J., Gao, Y., Guo, S., Hermann, J., Hermes, M. R.,  
317 Koh, K., Koval, P., Lehtola, S., Li, Z., ... Chan, G. K.-L. (2020). Recent developments  
318 in the PySCF program package. *The Journal of Chemical Physics*, 153(2), 024109.  
319 <https://doi.org/10.1063/5.0006074>
- 320 The HDF Group. (n.d.). *Hierarchical Data Format, version 5*. [https://github.com/HDFGroup/  
321 hdf5](https://github.com/HDFGroup/hdf5)
- 322 Tóth, G. (2003). An iterative scheme to derive pair potentials from structure factors and  
323 its application to liquid mercury. *The Journal of Chemical Physics*, 118(9). [https:  
324 //doi.org/10.1063/1.1543142](https://doi.org/10.1063/1.1543142)
- 325 Trott, C. R., Lebrun-Grandié, D., Arndt, D., Ciesko, J., Dang, V., Ellingwood, N., Gayatri,  
326 R., Harvey, E., Hollman, D. S., Ibanez, D., Liber, N., Madsen, J., Miles, J., Poliakoff, D.,  
327 Powell, A., Rajamanickam, S., Simberg, M., Sunderland, D., Turcksin, B., & Wilke, J.  
328 (2022). Kokkos 3: Programming model extensions for the exascale era. *IEEE Transactions*  
329 *on Parallel and Distributed Systems*, 33(4), 805–817. [https://doi.org/10.1109/TPDS.  
330 2021.3097283](https://doi.org/10.1109/TPDS.2021.3097283)
- 331 Valeev, E. F. (2024). *Libint: A library for the evaluation of molecular integrals of many-body*  
332 *operators over gaussian functions*. <http://libint.valeyev.net/>.
- 333 Velde, G. te, Bickelhaupt, F. M., Baerends, E. J., Fonseca Guerra, C., Gisbergen, S. J. A. van,  
334 Snijders, J. G., & Ziegler, T. (2001). Chemistry with ADF. *J. Comput. Chem.*, 22(9),  
335 931–967. <https://doi.org/10.1002/jcc.1056>
- 336 Zhang, L., Han, J., Wang, H., Car, R., & E, W. (2018). DeePCG: Constructing coarse-grained  
337 models via deep neural networks. *The Journal of Chemical Physics*, 149(3), 034101.  
338 <https://doi.org/10.1063/1.5027645>